How do climate and land use changes affect the water cycle? Modelling study including future drought events prediction using reliable drought indices

Article

Accepted Version

www.reading.ac.uk/centaur

CentAUR

Central Archive at the University of Reading

Reading's research outputs online

1   How the climate and land use changes affect the water cycle? Modelling study including the future

2   drought events prediction using reliable drought indices

3

4   Afzal, M.[1,2] and R. Ragab[1*]

5

6   **Abstract**

7   The two key factors that affect the water balance are climate and land-use changes. Although climate

8   change models have been developed for global scale, the implementation of their predictions is

9   commonly applied at catchment scale where the measurements are being carried out and the

10   management takes place. To investigate the impacts of climate and land use changes on the

11   hydrology, the Don Catchment in Yorkshire, UK, has been selected for this study. A physically based

12   distributed catchment-scale (DiCaSM) model has been applied. The model simulates the surface

13   runoff, groundwater recharge and drought indicators such as soil moisture deficit (*SMD*) and wetness

14   index (*WI*) of the root zone. The model was calibrated and validated against the observed river flow

15   and the model efficiency was evaluated using the Nash-Sutcliffe Efficiency factor (NSE). During the

16   calibration period (2011-2012), NSE was above 91% and during the validation period (1966-2012)

17   was above 83%. To study the impact of climate change on the streamflow and the groundwater

18   recharge, UK Climate Projections (UKCP09) data was applied. Under current land use changes under

19   different climate scenarios, the greatest decrease in streamflow and groundwater recharge is projected

20   under medium and high emission scenarios. Considering the projected increase in winter

21   precipitation, the increase did not contribute much into the streamflow and groundwater recharge due

22   to prolonged drier summer and higher temperature during the summer and autumn seasons that

23   resulted in an increase of evapotranspiration and soil moisture deficit (*SMD*). Climate change

24   scenarios projected an increase in evapotranspiration, soil moisture deficit more importantly in the

25   latter half of the current century and resulted in more extreme and severe drought events in

26   comparison to the baseline period. To study the impact of land use changes on water balance,

[1] Centre for Ecology & Hydrology (CEH), Wallingford, Oxfordshire, OX10 8BB, UK
[2] School of Earth and Ocean Sciences, Cardiff University, Main Building, Park Place, Cardiff, CF10 3AT
*Corresponding Author, R. Ragab, rag@ceh.ac.uk

27   different possible scenarios were created. The increasing of woodland had the most significant impact

28   by reducing the stream flow by up to 17% and groundwater recharge by 22%. Urbanization, could

29   lead to increase in stream flow and groundwater recharge. The magnitude of the impact of the climate

30   change was much more significant than the land use change on the streamflow and the groundwater

31   recharge. All the applied drought indices (*SMD*, *WI*, and *RDI*) identified an increase in the severity of

32   the drought under future climatic change scenarios, especially under high emission scenario where the

33   severity was the highest. Findings of the study are of great importance for Don Catchment that has 23

34   reservoirs for water supply. Some measures were suggested for sustainable management of the land

35   and water resources in order to meet future water demand in the light of diminishing water supplies.

36   **Key words:** Climate change, Land use change; DiCaSM Hydrological model; Don Catchment;

37   Reconnaissance Drought Index (RDI); Soil moisture deficit (SMD) and land-use change.

38

1. Introduction

Changes in the land surface hydrology are attributed to the collective effects of the changes in the climate, changes in vegetation, and the soil (Wang et al., 2018). Therefore, it is important to understand the impact of climate and land use changes on the water resources availability. In the UK, the land surface has changed slightly due to human interventions that mainly resulted in changes in land use for the food production, energy, housing and recreation. The recent land use changes are probably happening faster than at any other time in the human history, due to increase in demand for the natural resources, rapid changes in urbanisation, an increase in water demands for domestic and agricultural use. This is very significant for the UK where two-thirds of the land area is grassland. Approximately 14% of the UK is urban land which has significantly increased (by 300,000 hectares) since 1998 (Rounsevell and Reay, 2009). The other key land use changes are the agricultural land use practices which are driven by the farmers' decisions, which are economically driven by the availability of investment and subsidies (Shiferaw et al., 2009).

The UK and the study area (North East of England) have experienced a number of droughts, the most severe one is the one of 1976 (Marsh and Green, 1997). Annual precipitation in the region varies significantly, from 600 mm in the eastern lowlands to 2000 mm in western Pennine sites (Fowler and Kilsby, 2002). Contrary to the water supplies in the South-East region, water supplies in the North East depend on the reservoirs which fill during the winter months and are drawn down during the summer, this suggests that the water supplies in the region are more vulnerable to drought which is evident from the 1995 drought event (Fowler and Kilsby, 2002). The studied catchment, the Don is very significant for the water supplies in the region as there are 23 reservoirs within the catchment boundary which are recharged mainly during the winter months. Therefore, the main types of physical modification that affect the Don Catchment are the water storage and supply reservoirs, flood management structures, urbanisation and recreation including navigation (The Don Network, 2018).

The historic long-term record of the climate variables for the Sheffield area (part of the Don catchment area), covering the period from 1883 to 2015, suggests a significant annual warming trend (1.0 °C per

66   century), combined with an increase in annual precipitation (69 mm per century) with no significant

67   trend in seasonal precipitation (Cropper and Cropper, 2016). There is a general perception that the

68   urbanisation possibly added urban heat which contributed to the long-term warming trend which

69   resulted in extreme precipitation events. This could potentially affect the water resources availability in

70   the future and increase the drought risk, as water supplies within the catchment significantly depend on

71   the reservoirs. Considering the historic climate and land use changes and likely changes in the future,

72   it is important to study of the impacts of climate and land use changes on the studied catchment.

73   Although a number of studies including (Burke et al., 2010, Jackson et al., 2015, Wilby et al., 2015,

74   Spraggs et al., 2015) have been carried out to identify the historic droughts in the UK using the observed

75   data, less focus has been given to study the drought risk over catchment scale under different climate

76   and land use change scenarios and their impacts on water resources. This study aims to address this

77   issue in more detail and will also apply a number of indicators for the historic and future climate change

78   which could potentially be used as drought indicators to identify meteorological, agricultural and

79   hydrological droughts. The limited availability or access to the aquifers, the surface water reservoirs

80   significantly contribute to the water supplies of the studied area. As the water available in the reservoirs

81   is vulnerable to climate change, the reliability of water resources availability in the catchment could be

82   at higher risk due to the climatic variability.

83   The objectives of this study is to quantify the impact of climate and land use changes on catchment

84   water resources availability (surface and groundwater) and to develop suitable drought indicators to

85   predict future drought events.

86   Findings of the study are importance for the Don catchment for managing the water abstraction,

87   improvement in water infrastructure and planning for the future drought risk under climate change.

88   **2. Background of the studied catchment**

89   The Don Catchment (NRFA no. 27006) is in the North East of the country with a catchment area of 373

90   km^2 (Fig. 1). The naturalised discharge (where the river-flow was adjusted to take into account

abstraction and discharge into the river) was obtained from Environment Agency. This was needed as

streamflow is affected by presence of the 23 reservoirs, river abstraction for agricultural and industrial

use, groundwater abstraction and by treated wastewater discharge. The key land uses of the catchment

are: woodland which covers 15.8% of the catchment area, arable land, 6.1%, grassland, 35.6%, heather

area, 18.9% and urban area, around 14.0% (Fig. 2). The catchment contains a moderate permeability

bedrock which almost covers half of the catchment. Based on historical data, the average annual rainfall

for the Don Catchment is around 1085 mm and average temperature 7.8°C for the baseline data, 1961-

1990, the average annual rainfall for the studied period 1991-2012 was 1089 mm and the average

temperature 8.5 °C. The Don catchment is important for drinking water as it supplies conurbations of

South Yorkshire. Therefore, protecting drinking water sources now and in the future is essential. There

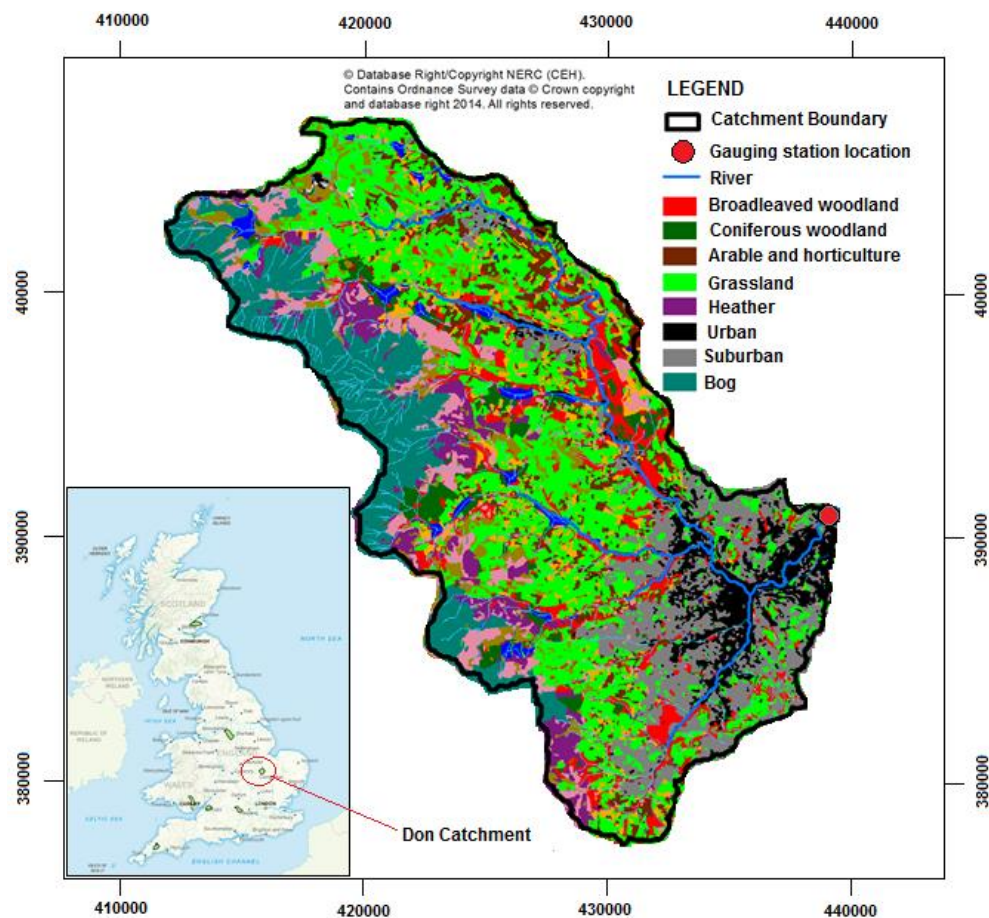are over twenty Yorkshire water reservoirs in operation.

Figure 1: The Don Catchment: boundaries, land use practices and location of the gauging station,
adapted from Morton et al. (2011).

3. Data, and the methodology

3.1. *Historic climate, soil, river flow and future climate data*

The Distributed Catchment Scale Model, DiCaSM model was run on a daily time step and spatial scale of 1 km^2 grid square area. The catchment area is 373 km^2 covered by 435 grid squares (as not all the grid squares were covered in the catchment boundary), each of which has 1 km^2 area. The model input requires a number of daily climatic variables including precipitation, temperature, wind speed, daily net radiation or total radiation and vapour pressure. Climate data were obtained from the Climate Hydrology and Ecology research Support System (*CHESS*) that accounted for the impact of changes in elevation on climatic data (Robinson et al., 2015, Tanguy et al., 2016). The historic continuous climatic variables and river flow data were available from 1961 until 2012. The catchment boundary and gauging station location data were available from Centre for Ecology and Hydrology (Morris et al., 1990, Morris and Flavin, 1994) and National River Flow Archive provided data for the daily river flow for the catchment (NRFA, 2014). The river and water body data were collected from the Centre for Ecology and Hydrology, 'Digital Rivers 50 km GB' Web Map Service (CEH, 2014). The UK Land cover data were obtained from the Centre for Ecology and Hydrology (Land Cover Map 2007, 25m raster, GB) Web Map Service (Morton et al., 2011). The soil data was obtained from the Cranfield University, (1:250 000 Soilscapes for England and Wales Web Map Service).

To study the impact of future climatic change on water supply systems, the UK Climate Projection Scenarios (UKCP09) was used using the joined probability factors and the UKCP09 weather generated data. In this study three 30-year periods: 2020's (2010-2039), 2050's (2040-2069) and 2080's (2070-2099) for the three greenhouse gas emission scenarios (low, medium and high) were considered. In UKCP09, Bayesian probability is used in which probability is derived from observations and outputs from a number of climate models, all with their associated uncertainties. The UKCP09 provides monthly, seasonal and annual, probabilistic changes factors at 25 km by 25 km grid square resolution for precipitation and temperature (Table 1). The seasonal temperature shows an increase in emissions scenario and time, particularly in summer and autumn, whereas the precipitation is showing rainfall

decreases in summer and increases in winter relative to the 1961-1990 'baseline' period. The weather generator, WG, of UKCP09 provides daily output data at a 5km^2 resolution for more climate variables such as vapour pressure and sunshine hours, in addition to rainfall and temperature. This data was downscaled using the weighing factors from (*CHESS*) methodology that accounted for the impact of changes in elevation on climatic data. The sunshine hours were converted into net radiation following the methodology of Allen et al. (1998). For the initial exploratory analysis, simplified change factors were derived from UKCP09 joint probability central estimates. The joint probability plot was used to generate seasonal climatic change factors (% change in rainfall and change in temperature, ± °C) to apply as an input to the DiCaSM model.

Table 1: Probabilistic changes in temperature and precipitation for the Don Catchment under UKCP09 climate change scenarios (joint probability) under three emission scenarios and three selected time periods.

		Low emissions				Medium emissions				High emissions			
		Winter	Spring	Summer	Autumn	Winter	Spring	Summer	Autumn	Winter	Spring	Summer	Autumn
Change in temperature (°C)	2020s	1.3	1.3	1.5	1.6	1.4	1.3	1.4	1.5	1.4	1.3	1.4	1.6
	2050s	2.0	1.7	2.2	2.3	2.1	1.9	2.0	2.6	2.6	2.3	2.4	2.7
	2080s	2.4	2.2	2.1	2.7	2.7	2.8	3.0	3.3	3.5	3.5	3.8	4.3
Change in precipitation (%)	2020s	4.7	2.2	-6.8	3.2	4.1	1.6	-6.5	2.2	4.8	1.3	-7.3	2.4
	2050s	8.0	1.2	-16.3	1.9	8.5	0.6	-14.8	4.1	9.8	0.7	-16.5	5.0
	2080s	9.6	1.3	-13.4	3.5	11.8	1.5	-20.1	4.6	16.8	1.5	-28.2	5.0

Time period →

Increased greenhouse gas emissions →

For the detailed weather generator simulations, 100 realizations of the daily time series data were generated in order to account for the uncertainty associated with the scenarios and alternative timing of events. This data was subject to bias correction, which was carried using the '*qmap*' package in R statistical tool (Gudmundsson et al., 2012) using the 1961-1990 observation data as a reference period. This method has been successfully applied in drought studies including the study of Wang and Chen (2014). Forestieri et al. (2018) applied this bias correction method to study the impacts of climate

change on extreme precipitation in Italy, De Caceres et al. (2018) subjected the daily climate models data to this approach and recently Hakala et al. (2018) applied this bias correction method to evaluate climate model simulations.

3.2. *Historic land use and its importance*

The studied Don catchment is not only significant for agriculture but also significantly contribute to the domestic water supplies. Water supplies in the catchment area come from the twenty-three reservoirs which are located within the catchment boundary. The low river flow can affect navigation, water supplies, and the aquatic ecosystem. Low flow also can result in river pollution due to the low dilution of the sewage effluent and can affect aquatic systems resulting in reducing the recreational activities within the catchment. Agriculture census data reveals that the key land-use in the area is grassland, heather and urban, with less than 10% of the catchment being agriculture (Fig. 2).
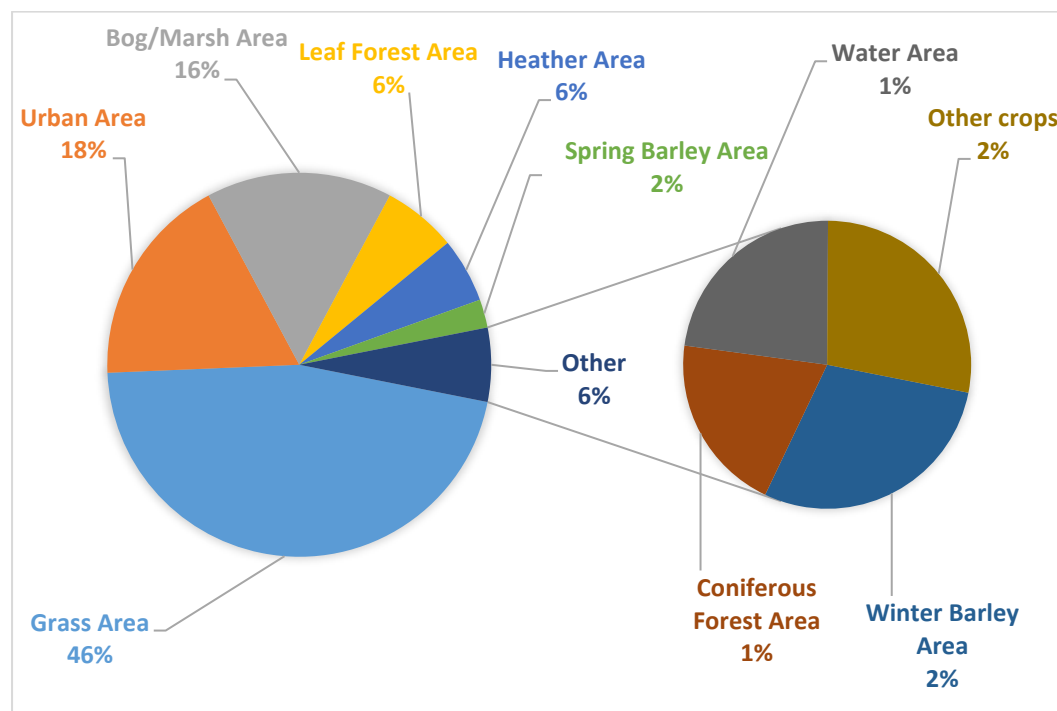

Figure 2: Current land use in the Don catchment

3.3. *Schematic representation of modelling work*

The schematic representation of the modelling work is shown in Figure 3 which shows the data sources used in the study. Both historic and future climatic variables data were used to generate the streamflow,

168 groundwater recharge, net rainfall, potential and actual evapotranspiration, soil moisture deficit (*SMD)*,

169 wetness index (*WI)* of the root zone and water losses due to interception. All these variables were

170 directly or indirectly used to calculate the drought risk for both the historic period and for future climate

171 change scenarios. Methodology about each used drought index is discussed later.

172
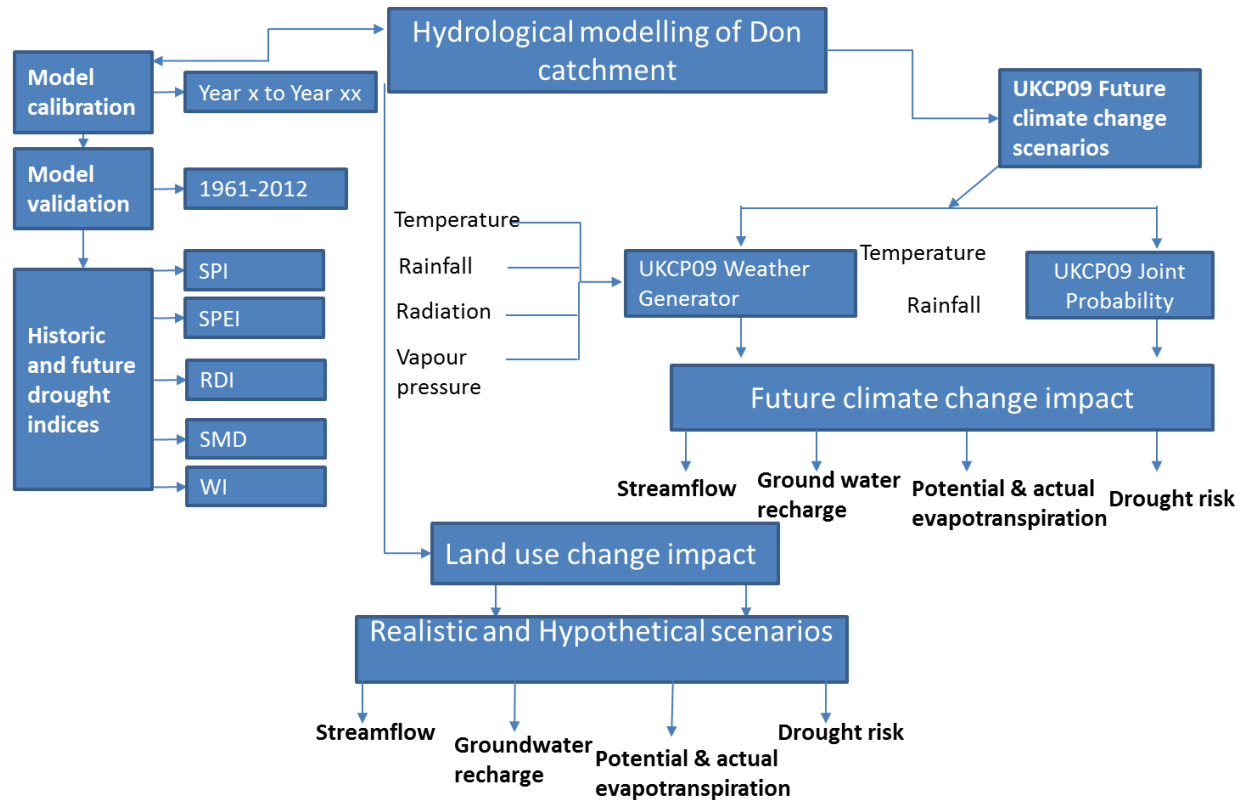
Figure 3: Schematic representation of the modelling application

3.4. *DiCaSM model input data and processes*

175 The hydrological DiCaSM is the acronym for the Distributed Catchment Scale Model was used to

176 simulate the water balance of the catchment. The key input of the model are the meteorological data

177 (temperature, rainfall, net radiation or total radiation, vapour pressure and wind speed), land use and

178 vegetation (up to 20 land-uses can be assigned per each grid square), land altitude/elevation using the

179 Digital Terrain Model, DTM, vegetation parameters and soil physical properties of each soil layer

180 (saturated soil moisture content, soil moisture content at field capacity, soil moisture content at wilting

181 point, saturated hydraulic conductivity). The model runs on daily time step and produces an output

182 including spatially and temporally distributed series of potential evapotranspiration, actual

183 evapotranspiration, soil water content, soil moisture deficit (*SMD*), wetness index (*WI*) of the root-

184 zone, groundwater recharge, streamflow and surface runoff (Ragab and Bromley, 2010). The model is

185 capable of simulating the impact of the changes in climate and land use on the catchment water balance.

186 The model also addresses the heterogeneity of input parameters of soil and land cover within the grid

187 square using three different soil and plants algorithms (Ragab et al., 2010). In the model, runoff is routed

188 between the low points of each grid square along the prevailing slope using the digital terrain model

189 (DTM).

190 The model simulates the following processes, rainfall interception by land cover, evapotranspiration,

191 surface runoff, infiltration, groundwater recharge, plant water uptake, bare soil evaporation and stream

192 flows. Further details about the model are given in Ragab et al. (2010) and Ragab and Bromley (2010).

193 For the studied catchment, the vegetation parameters (plant height, Leaf Area Index (*LAI*), and the

194 canopy resistance were obtained from the UK-MORECS system (Hough et al., 1997). The model's

195 efficiency (goodness of fit), measured during the model calibration and validation, was carried out using

196 several efficiency indices, including Nash-Sutcliffe Efficiency (NSE), log of Nash-Sutcliffe Efficiency

197 (log NSE) and Coefficient of Determination, R^2 as given below.

198 *3.4.1 Indices of measuring the model efficiency*

199 The calibration procedure consisted of adjusting the parameters related to stream flow calculations to

200 achieve the best model fit, assessed using the *NSE* and log *NSE* of the stream flow. To estimate the

201 model efficiency/goodness of fit , modelled and observed flow data were compared using a number of

202 indices, including the Nash-Sutcliffe Efficiency (*NSE*) coefficient (Nash and Sutcliffe, 1970). *NSE* is

203 the most widely used coefficient to assess the performance of stream flow (Gupta et al., 2009), the value

204 of 100% indicating a perfect match.

205 $$NSE \ = 100 - \frac{\sum_{i=1}^{n}(O_i - S_i)^2}{\sum_{i=1}^{n}(O_i - \bar{O})^2} \qquad\qquad (1)$$

206   where O_i and S_i *refers* to the observed and simulated river flow data, respectively, and $\bar{O}$ is the mean of

207   the observed data. Another index "Log NSE" is commonly used for low flows and based on the stream

208   flow logarithmic values has also been considered, (Afzal et al., 2015, Krause et al., 2005). In addition,

209   the model performance was also evaluated using the statistical indicators namely Coefficient of

210   determination, R^2 as:

211    $$R^2 = \left\{ \frac{1}{N} \frac{\sum[(y_0 - \overline{y_0}] \overline{(y_s - \overline{y_0})}}{\sigma y_0 - \sigma y_s} \right\} \qquad\qquad (2)$$

212   where y_o is the observed value, y_s is the simulated value, N is the total number of observations, $\bar{y}_o$ is the

213   average measured value, $\bar{y}_s$ is the average simulated value, σy_0 is the observed data standard deviation

214   and σy_s is the simulated data standard deviation. The values of this index can range from 1 to 0, with

215   one indicating perfect fit.

216   *3.5 Identification of drought indices*

217   The main drought drivers are temperature, radiation, wind speed, relative humidity / vapour pressure

218   (Seneviratne, 2012). Figure 4 shows how these drought drivers can cause meteorological, agricultural

219   and/or hydrological droughts. A number of drought indices can be used to identify drought events. The

220   most common one is the Standardized Precipitation Index (*SPI*) (McKee et al., 1993). The SPI index

221   represents the deviation of precipitation from the long-term average, negative values indicate below

222   average "dry periods" and positive values indicate above average precipitation "wet periods". The index

223   helps in finding different types of droughts, as precipitation is the key climatic variable upon which soil

224   moisture deficit, stream flow and groundwater recharge depend. Therefore, it could easily be used to

225   quantify the severity of both dry and wet events. Another drought index is the standardized precipitation

226   evapotranspiration index (*SPEI*) which is a multiscale drought index, sensitive to global warming

227   (Vicente-Serrano et al., 2010). This index has been widely applied in different parts of the world

228   (Bachmair et al., 2018, Kunz et al., 2018) to the study meteorological and agricultural droughts and to

229   study the impacts of drought severity on vegetation health (Bento et al., 2018). The equation used to

230   calculate *SPEI* is based on (Thornthwaite, 1948):

11

231     $D_i = P_i - PET_i$ (3)

232   where Di is the difference between the precipitation (P) and the potential evapotranspiration (PET) for

233   a particular month. The aim of applying this index was to measure the water surplus or deficit for the
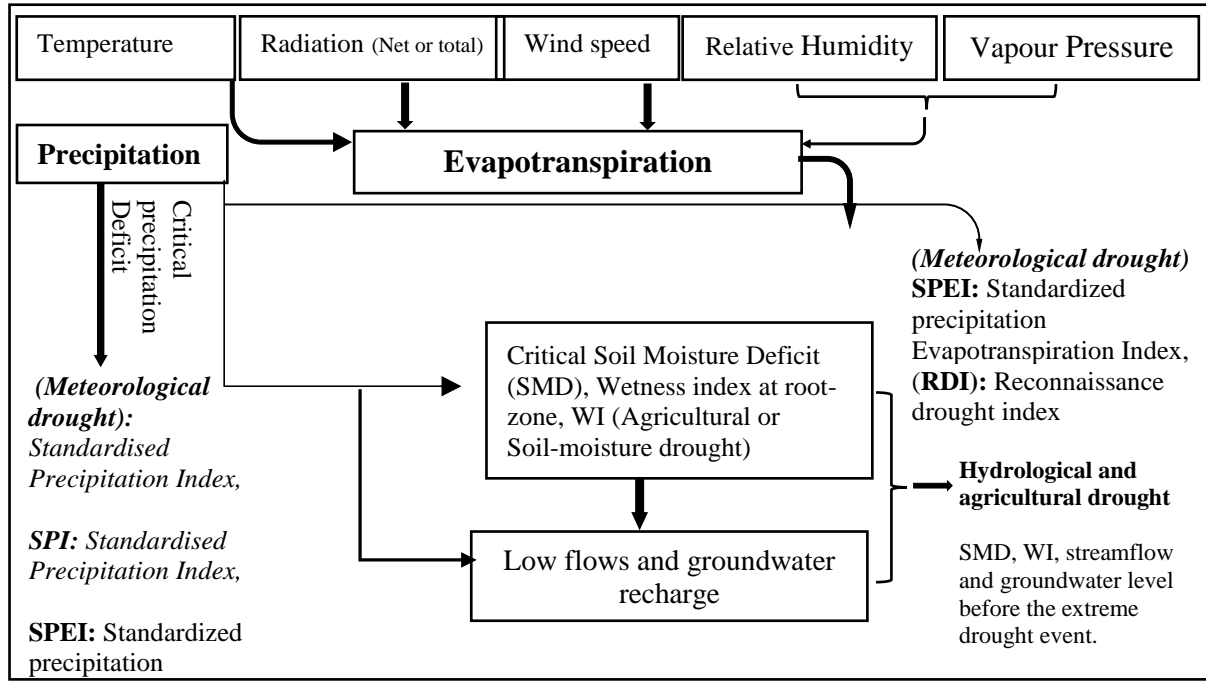
234   analysed month.

250   **Figure 4:** Key drought drivers of the meteorological, agricultural and hydrological droughts.

252   Like the *SPI*, a negative value shows dryness and a positive value shows wetness, relative to the long-

253   term average. This drought index has been applied in a number of studies for example (Tirivarombo et

254   al., 2018) and was used recently to study severity of extreme droughts events, like those of Cape Town,

255   South Africa (Solander and Wilson, 2018). Another key drought index used in this study was the

256   Reconnaissance Drought Index (*RDI*) which is based on Tsakiris et al. (2007). The standard RDI is

257   calculated using the ratio of precipitation to potential evapotranspiration over a certain period. It is a

258   good indicator for describing agricultural, hydrological and meteorological droughts. The

259   Reconnaissance Drought Index (*RDI*) was calculated as:

260     $a_0^{(i)} = \dfrac{\sum_{j=1}^{12} P_{ij}}{\sum_{j=1}^{12} PETorAE_{ij}}$ (4)

261 $$RDI_n^i = \frac{a_0^{(i)}}{\bar{a}_0} - 1 \qquad\qquad (5)$$

262 $$RDI_{st\,(k)}^i = \frac{y_k^{(i)} - \bar{y}_k}{\hat{\sigma}yk} \qquad\qquad (6)$$

263 where P_{ij} and PET_{ij} are the precipitation and potential evapotranspiration of the j_{th} month of the i_{th}

264 hydrological year (starting from October), is $\bar{a}_0$ the arithmetic means of the a_0 calculated for the

265 number of years. In the above equation y_i is the ln $(a_0^{(i)})$, $\bar{y}_k$ is its arithmetic mean and $\hat{\sigma}yk$ is its

266 standard deviation. This drought index has been used in studies in different parts of the world,

267 including Greece (Vangelis et al., 2013) and Iran (2015). This method is widely accepted and applied

268 as it calculates the aggregated deficit between precipitation and the atmospheric evaporation demand.

269 The method is directly linked to the climate conditions of a region and is comparable to the FAO

270 Aridity Index (Tsakiris et al., 2007). In addition to the conventional way of calculating *RDI*, an

271 adjusted *RDI* was calculated using the net rainfall (gross rainfall minus rainfall interception losses by

272 canopy cover) and actual evapotranspiration. Further to *SPI*, *SPEI* and *RDI*, two other drought indices

273 were considered: the soil moisture deficit (*SMD*) and the wetness index (*WI*) of the root-zone (Ragab

274 and Bromley 2010). *WI* ranges from zero to 1. The value of 1 means the catchment is at its maximum

275 soil moisture content and 0 means the catchment at its lowest soil moisture content of the simulated

276 period (Kalma et al., 1995). Wetness Index of the root zone (scaled soil moisture calculated as

277 (current soil moisture – minimum soil moisture)/ (Maximum soil moisture – minimum soil moisture).

278 Using a range of drought indices helps in identifying different types of droughts (meteorological,

279 hydrological and agriculture), for example SPI for meteorological, *RDI* for hydrological and *WI* and

280 *SMD* for agricultural drought.

281 ## 4. Results

282 ### 4.1 *Model calibration/validation for the streamflow*

283 The key six model parameters that were used to calibrate the model against the observed flow data

284 were: the percentage of surface runoff flow routed to the stream, the catchment storage/time lag

285 coefficient, an exponent function describing the peak flow, a stream storage/time lag coefficient, a base

286 flow factor and the streambed leakage. The other factors on which model performance is also affected

287   by are the soil hydraulic properties and the land cover parameters. The selected time period for

288   calibration was run using a simple iteration algorithm for optimization in which each of the six stream

289   flow parameters was assigned a range described by a minimum and a maximum value. Each range was

290   divided into a number of steps and the number of total iterations is the product of multiplication of the

291   steps of the six key parameters. The number of iterations for each parameter was assigned according to

292   the parameter sensitivity, i.e. a higher number of iterations were assigned to parameters, which showed

293   more sensitivity to the streamflow. The model calculates the Nash-Sutcliffe Efficiency value, *NSE,* ln

294   NSE and R^2 for each iteration. The model optimisation process helps in finding a good set of parameters

295   that produces a good model efficiency value. Figure 5 (top) shows the model calibration during 2001-

296   2012 where model efficiency, measured using the Nash-Sutcliffe Efficiency, was above 87% with less

297   than two percent percentage error. The selected calibration period included a dry and a wet period in

298   order to assess the model performance during both conditions.

299   The model performed well both during the rainy and dry events and responded according to soil

300   hydrology status, i.e. during the soil moisture deficit period, a small rainfall event did not generate

301   enough streamflow and during the heavy rainfall event, when the soil was at saturation during the winter

302   months, the model responded extremely well. The model validation results during the drought period

303   are shown in Figure 5 (bottom) for the 1970s decade, during this period model efficiency measured

304   using the Nash Sutcliffe Efficiency was above 80%, which shows good confidence in the used model

305   efficiency parameters. The results of model prediction efficiency calculated in percentage as Nash

306   Sutcliffe Efficiency, ln Nash Sutcliffe Efficiency or R^2 values are shown in Table 2. The model

307   calibration was carried out over a shorter period and validation over a number of 10-year periods and

308   over the entire study period. The overall model performance over the whole period, 1961-2012 was

309   good, (NSE = 83%). The correlation between the observed and simulated flow of different time periods

310   is shown in Figure 6. The figure shows the model's capability to reasonably predict stream flows both

311   during the model calibration and validation periods for both dry and wet periods.

312

313   **Table 2:** Don Catchment model performance during the stream flow calibration and validation stages.

Periods	NSE	ln NSE	R^2	Square root of R^2	Average Modelled flow $m^3 s^{-1}$	Average Observed flow $m^3 s^{-1}$	% Error
2001-2012[*]	87.08	73.1	0.87	0.93	4.86	4.73	2.61
1991- 2000	87.03	79.1	0.88	0.93	5.10	5.18	-1.60
1981-1990	83.13	76.4	0.84	0.91	5.17	5.13	0.81
1971- 1980	82.21	66.1	0.83	0.91	4.68	4.90	- 4.63
1966-2012	83.06	73.0	0.84	0.91	5.06	5.08	-0.60

314   *calibration period

315

316

317
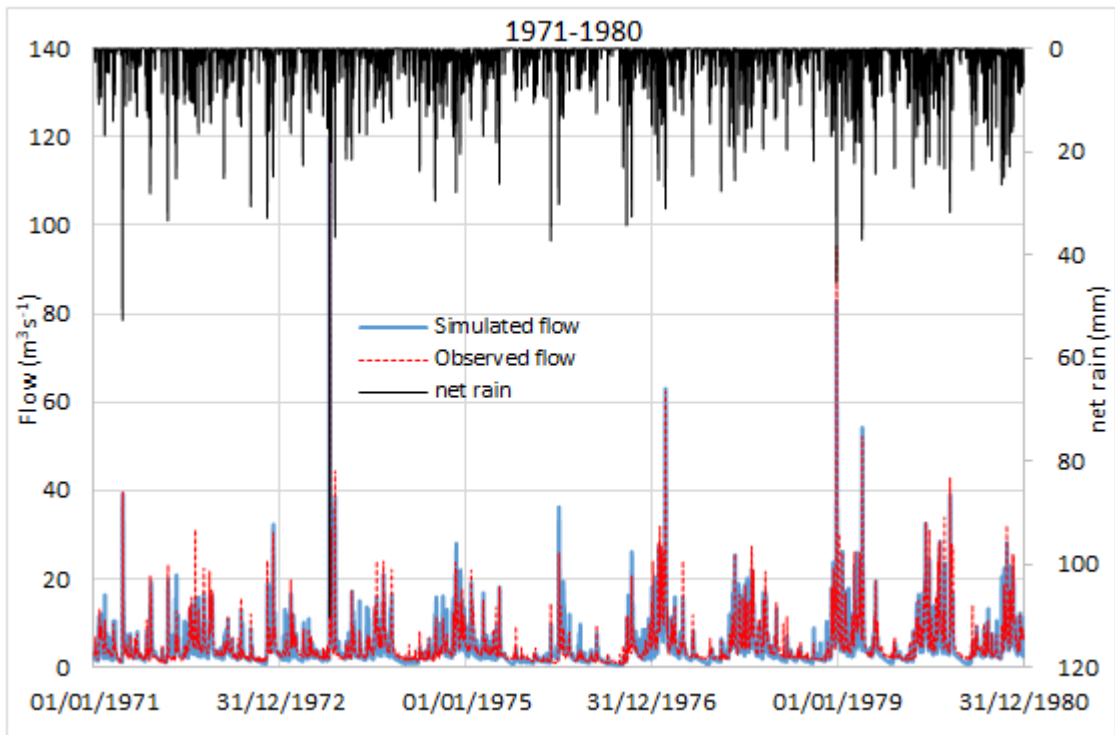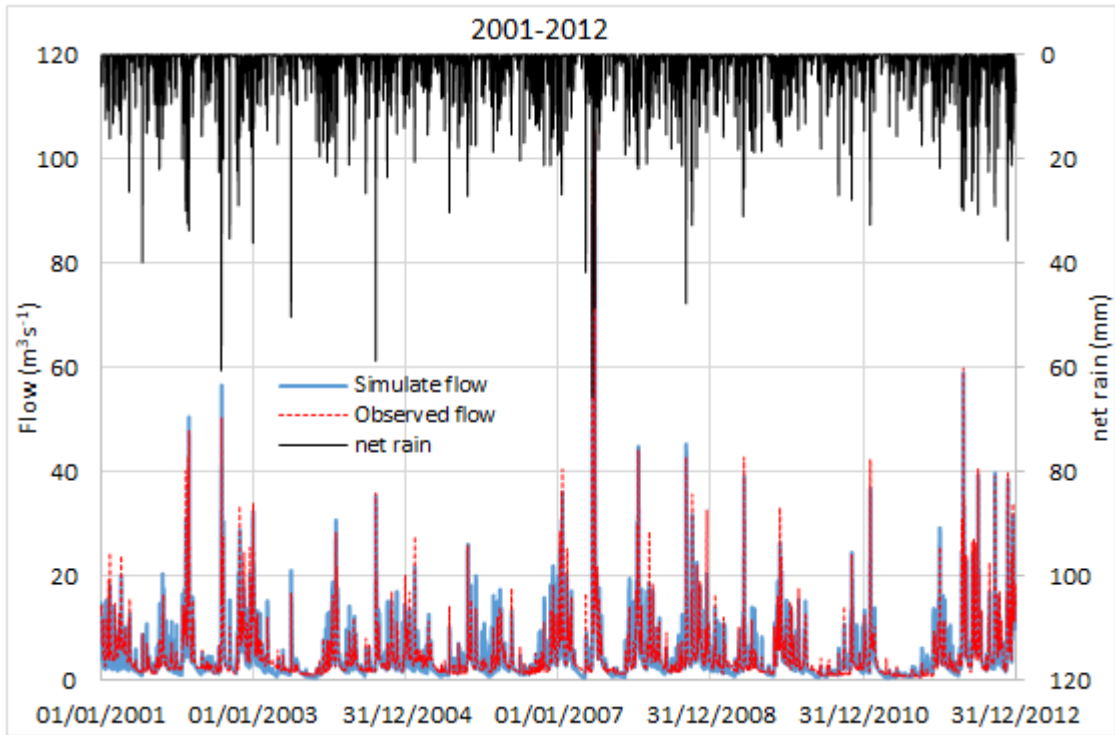
318
319 **Figure 5:** Don Catchment calibration (2011-2012) and validation (1971-1980) period.
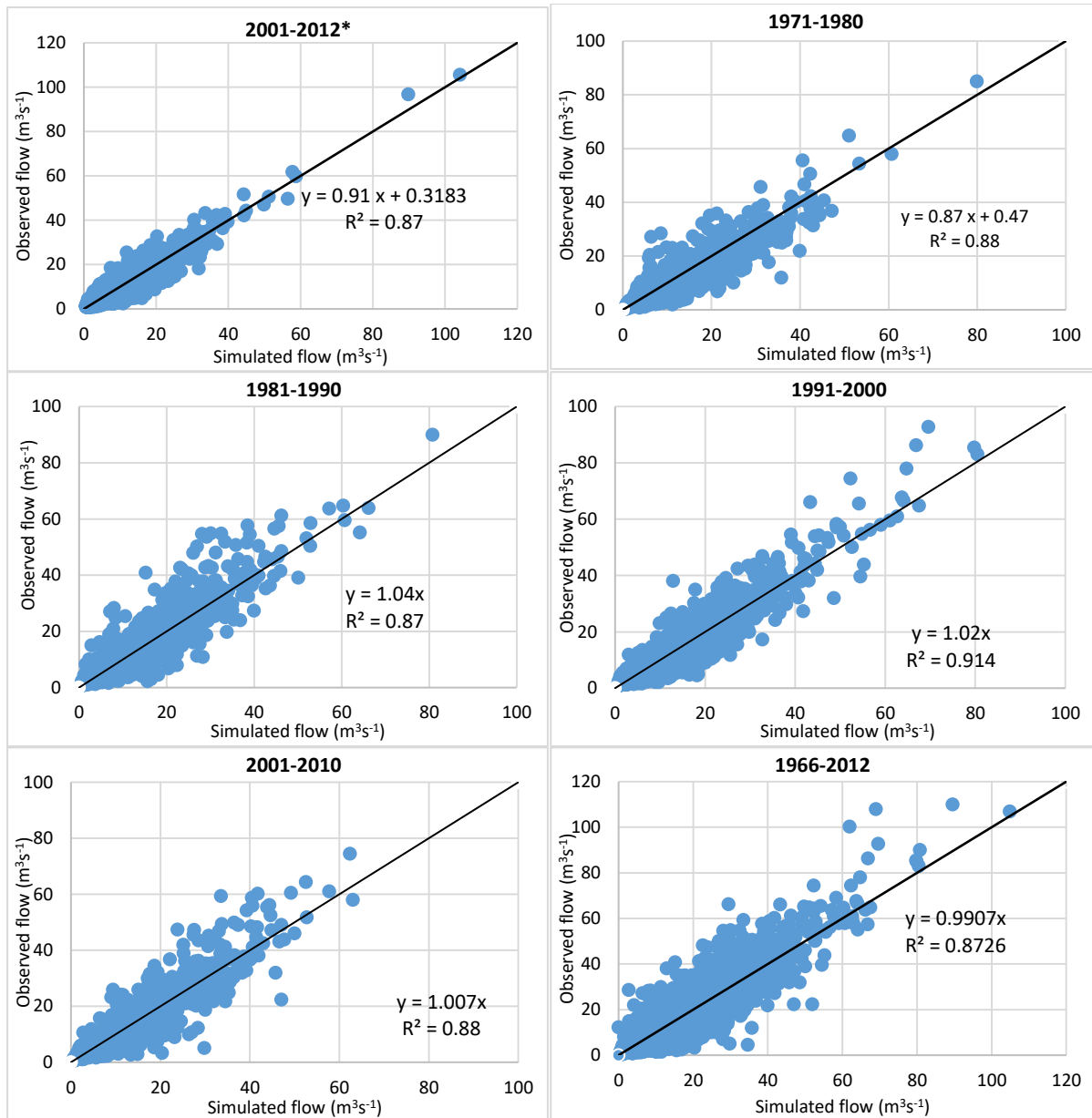
320

321

322

323
324 **Figure 6:** Relationship between the observed the simulated flow during the model calibration and

325 model validation over a decadal time scale and over the entire period.

326 ***4.2 Identification of historic droughts***

327 *4.2.1 The standardized precipitation index (SPI) and Standardized Precipitation Evapotranspiration*
328 *Index (SPEI)*

329 The *SPI* is the most commonly used drought index to describe the deviation of the precipitation from

330 the average precipitation. The *SPI* index scale values mean: above 2.0 extremely wet, 1.5-1.99 very

331 wet, 1.0 -1.49 moderately wet, -0.99 to 0.99 near normal, -1.0 to -1.49 moderately dry, -1.5 to -1.99

severely dry and -2.0 and less, extremely dry (McKee et al., 1993). The SPI and SPEI time series are shown in Figure 7 which also illustrates that the SPEI has shown higher severity for both dry and wet events, more clearly for the 1970s drought. Both indices picked up all the drought events which took place in the Don Catchment between 1961 and 2012.
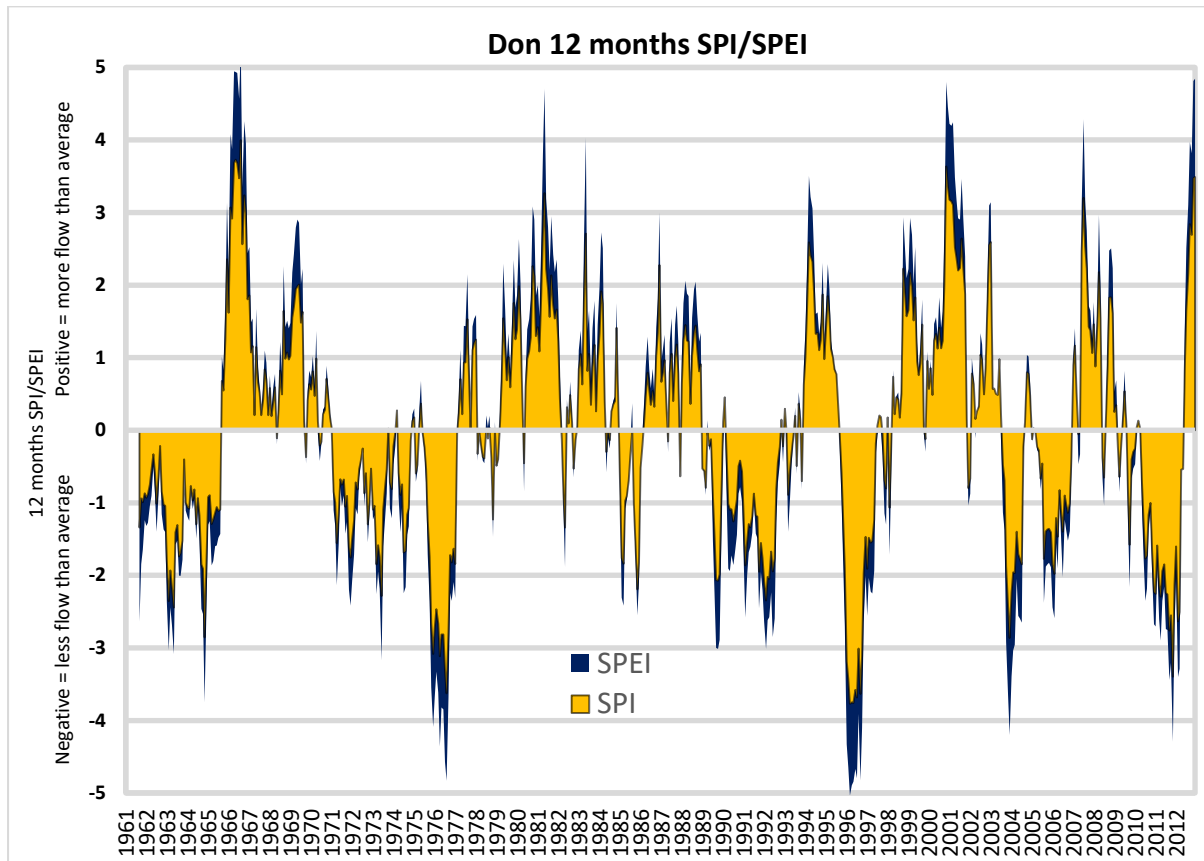

Figure 7. The standardized precipitation index (SPI) and standardised precipitation potential evapotranspiration index (SPEI) of the Don Catchment from 1961 to 2012.

As the evapotranspiration calculation in the model is dependent on climatic data as well as on a number of soil and plant parameters, the *SPEI* is expected to better represent the severity of the drought. Both *SPI* and SPEI indices crossed over the 'extremely severe' drought level during the most well-known 1970s drought which affected most parts of the UK and Europe. The catchment experienced two extreme drought events which took place in the mid-1970s and the mid of 1990s. These drought indices show that the Don Catchment was subjected to drought events which significantly affected Southern England, the Anglian regions, Southern and Eastern England and the Midlands (Parry et al., 2016). The drought termination rate showed a west-east divide in 1995-1998, which was more apparent in the

18

347   Midlands and Southern and Eastern England. This is evident from both the *SPI* and *SPEI* indices, which

348   crossed over the 'extreme drought' level during both the 1970s and the 1990s droughts. Not only the

349   occurrence of the drought events (frequency) but also the duration and drought strength significantly

350   affect the streamflow and the groundwater recharge.

351   Therefore, the *SPI* and *SPEI* indices could be used as good indicators for the meteorological and

352   hydrological drought. The *SPI* and *SPEI* indices over 52 years elucidated the successive dry events, like

353   those occurred in the 1970s and the 1990s. The *SPI* and *SPEI* indices also help in identifying smaller

354   magnitude drought events, or drier periods, which took place in the late 1960s, early 1990s, in 2005-

355   2006 and in 2010. The magnitude of the severity of drought was considered as severe in the mid-1970s,

356   in 1976 and in 1996 when *SPI* and *SPEI* indices were well below -2, 'extreme drought' level.

357   4.2.2. *Reconnaissance Drought Index (RDI)*

358   Figure 8 shows the comparison between the adjusted *RDI* and the classical RDI. Both picked up all the

359   drought events, which were detected by the *SPI*. However, the advantage of applying the *RDI* over SPI

360   is that it does not rely on one factor only, i.e. precipitation. The adjusted *RDI* showed slightly different

361   severity levels, especially during the extreme drought events. In addition, there is a strong correlation

362   between the two ways of calculating the *RDI* and the *SPI/SPEI*. Figures 7 and 8 show that the extreme

363   drought conditions of 1976, 1996 and 2006 was picked up similarly by both *SPI/SPEI* and *RDI/adjusted*

364   *RDI*. Drier than average events (*SPI*/SPEI less than -10% or *RDI* less than -1) were also observed in

365   1964, 1975, 1990, 1996, 2003, 2005, 2011. Both drought indices also picked up extreme drought events

366   which took place in 1976, 1989 and1996. However, the severity of the drought event was slightly higher

367   when applied reconnaissance drought index using the gross rainfall and the potential evaporation in

368   most of the cases. Based on both types of RDIs and SPI/SPEI drought indices, the total percentage of

369   wet years were higher than total percentage of dry years.
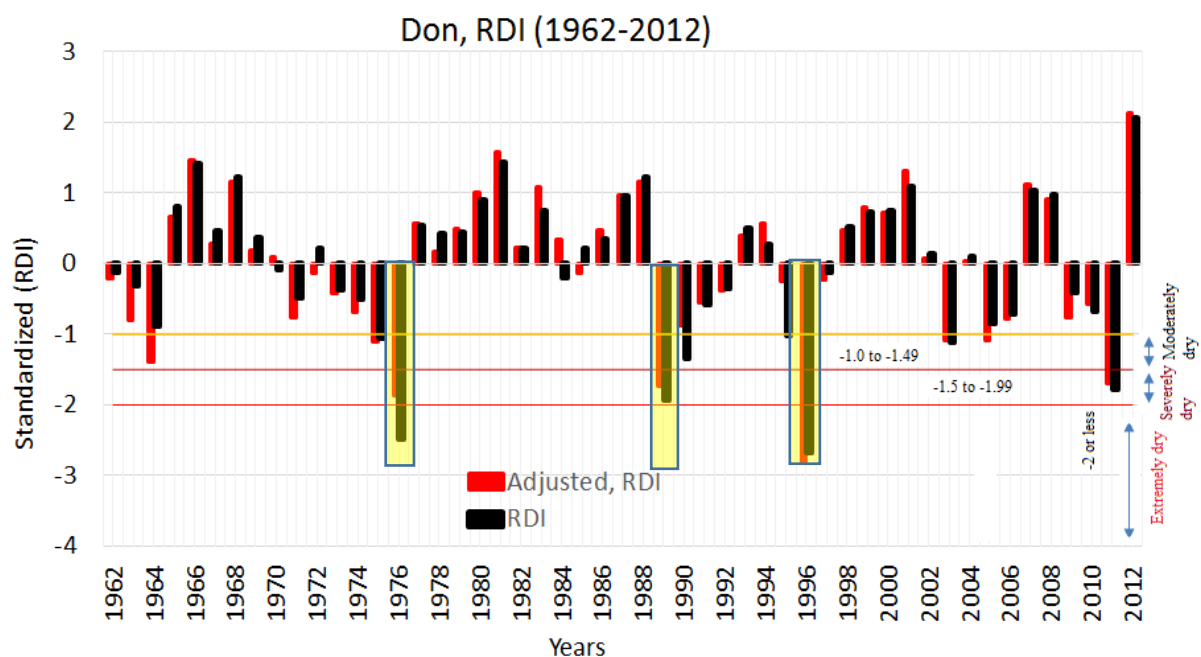
Figure 8: Standard RDI (Reconnaissance drought index) based on potential evapotranspiration and total rainfall and the adjusted RDI, calculated using net-rainfall and actual evapotranspiration, for the Don Catchment during the 1962-2012 period.

4.2.3. Soil moisture deficit, *SMD* and Soil Wetness Index, *WI* as a drought indicator

In addition to the *SPI/SPEI* and *RDI* drought indices, which are more commonly used to predict meteorological and hydrological droughts, two other drought indices soil moisture deficit and wetness index of the root-zone, which are more appropriate for the agriculture drought, were applied in the study. For agriculture drought, the soil moisture deficit, *SMD* and the wetness index, *WI* of the root-zone are more appropriate (Fig. 9). The wetness index, *WI* represents how relatively wet or dry the catchment is over the period.

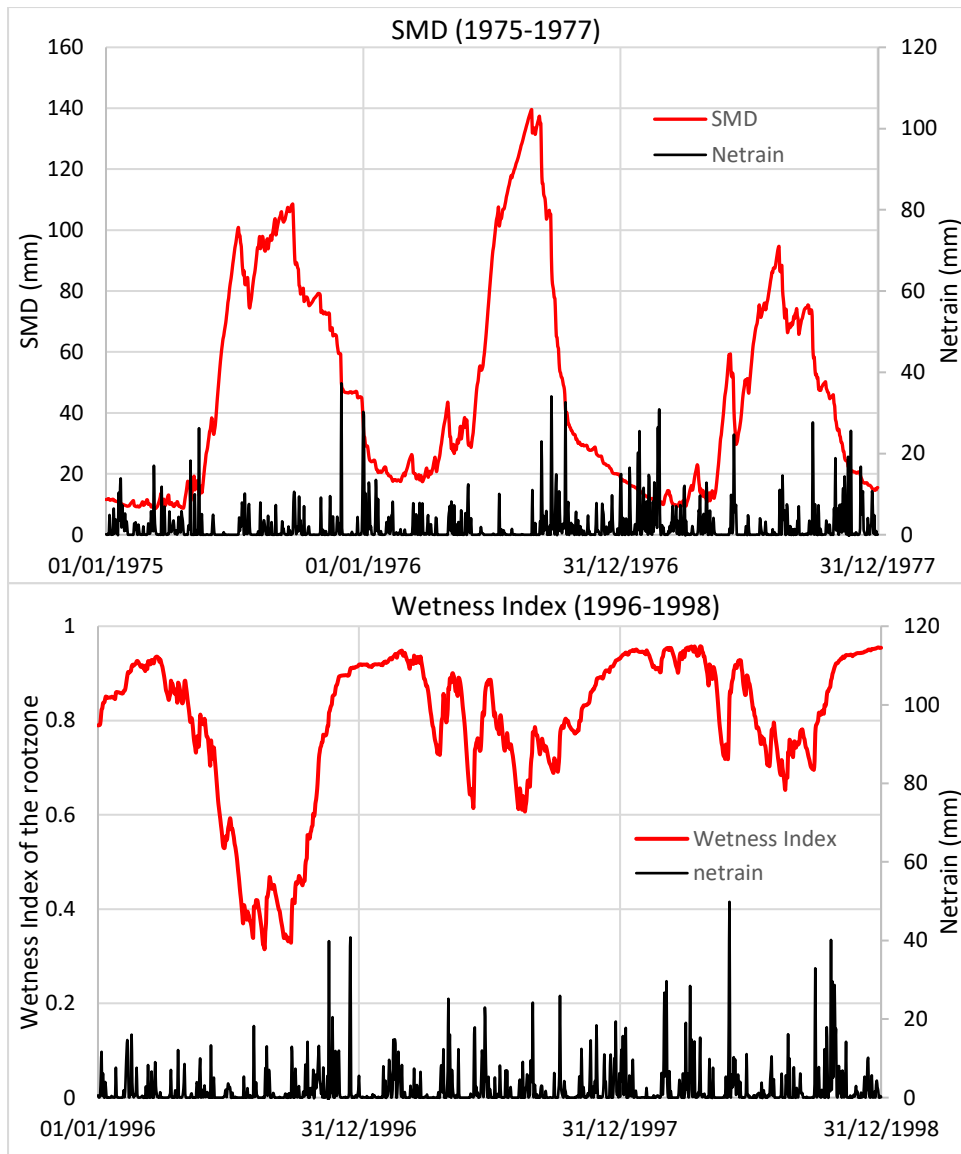**Figure 9:** Soil moisture deficit from 1975 to 1977 (top) and Wetness Index of the root-zone from 1996 to1998 (bottom) for the Don Catchment.

The WI is a scaled soil moisture status that accommodates the spatial variability of soil types, elevation, vegetation cover, etc. across the catchment. The Soil Moisture Deficit, *SMD* represents the deviation of soil moisture from the soil moisture at field capacity. Here zero means, the catchment's soil moisture is at field capacity level. The deviation gets larger when the soil moisture starts to fall below the field capacity, especially during summer and during drought periods. Examples of both indices are shown in Figure 9 which clearly shows the significant change in soil moisture indicators *WI* and *SMD* during the dry summer months, especially during the extreme droughts in 1975 and 1976 and the recovery in 1977 for the SMD. In the dry summer months of 1975, the soil moisture deficit exceeded 100 mm and during the 1976 dry summer period, soil moisture deficit was over 140 mm. The figure also shows the severity

422 of the dry spell as a result of the continuation of the dry seasons including the 1975-1976 winter months

423 as the *SMD* did not drop down to zero, whereas in the 1977 winter months, above average winter rainfall

424 brought the *SMD* back to zero after persistent rainfall events during the 1977 winter months. It can also

425 be seen that the *WI* dropped below the winter value of 1.0 to 0.3 during the extreme drought of the

426 summer of 1976 and mirrored the other drought indices including the SPEI/SPI and the RDI.

427 ### *4.3. Future climate change impact on the water resources*

428 #### *4.3.1 Changes in streamflow*

429 The future climate change scenarios (UKCP09) suggest an increase in temperature under all emission

430 scenarios and a decrease in rainfall, during the summer months (Table 1). To study the impact of climate

431 change on the hydrology of the Don catchment, the future climate projections were derived using two

432 approaches based on UKCP09 outputs: simplified change factors based on joint probability data and

433 the weather generator data. Using the joint probability approach, nine scenarios (three time periods and

434 three emission scenarios) were investigated. The seasonal climate change factors (relative to the

435 baseline data, 1961-1990) of temperature (± change in °C) and rainfall (% change in rainfall) at the

436 most likelihood (central estimate) probability level were input into the DiCaSM model and applied on

437 the 1961-1990 baseline climate data (Table 1).

438 A significant change in streamflow was observed using both approaches. The simplified change factor

439 (joint probability) approach suggests that streamflow is likely to increase in winter (December, January,

440 February) by up to 10% in the 2080s under high emission scenarios due to an increase in winter rainfall.

441 Similar results were also observed using the weather generator data for the winter months, but the

442 decrease in streamflow was not that significant (Fig. 10). This is of greater significance for the Don

443 Catchment which significantly contributes to the water supplies in the region as there are 23 reservoirs

444 within the catchment boundary which are recharged mainly during the winter months.

445 In the spring (March, April, May) season, there is little difference in the change in streamflow under

446 three emission scenarios and three selected time periods. With an exception in the 2020s, under low and

447   medium emission scenarios, where the streamflow in spring is likely to decrease by -2.11% to -5.45%

448   under low emission scenarios, -1.48% to -4.82% under medium emission scenarios and within -1.39%

449   to -4.45% under high emission scenarios, relative to the baseline period. During the spring season, the

450   evaporation is low relative to the precipitation and the soil is more saturated except during the latter

451   part of spring (Fig. 10).

452   During the 2020s period, in summer, a significant decrease in streamflow is projected under all emission

453   scenarios. In the 2020s, the summer streamflow is likely to decrease, by 13 to15 % using the joint

454   probability approach, whereas under the weather generator only a small decrease of up to 4.5% is

455   projected. In 2050s a significant decrease of 12.75 to 17.86 % relative to baseline period is projected

456   using the weather generator data, whereas under the joint probability, a decrease is projected from 27

457   to 29 % with no significant variation under different emission scenarios. During the summer season in

458   the 2080s, using the joined probability approach, the stream flow is likely to decrease by 24 to 42%,

459   whereas using the weather generator data, streamflow is likely to decrease by 16.05 to 25.5%, depending

460   on the emission scenario.

461   The severity of the change, particularly during the summer season, could lead to very low stream

462   flows, possibly leading to a high risk of inadequate domestic, industrial and agricultural water supply.

463   The latter is more significant for the Don catchment, as river water abstraction is very significant. The

464   streamflow is likely to decrease in the summer season because the soils are not saturated like they are

465   during winter and spring, as a results soil moisture deficit is likely to increase. The combined effect of

466   decreasing rainfall with the increasing temperature could result in higher evapotranspiration during

467   the summer season, which in turn could result in reduced flow especially under high emission

468   scenarios. This is because the temperature is likely to increase by 4.6 ^{0}C and rainfall to decrease by up

469   to 34% by the end of the century. The relationship between the precipitation and the hydrological

470   response is much more dependent on antecedent catchment conditions. With reductions in

471   precipitation in autumn and spring (enhanced by higher evaporation), saturated conditions will occur

472   less frequently, and precipitation events will be less likely to generate high runoff flow flows.
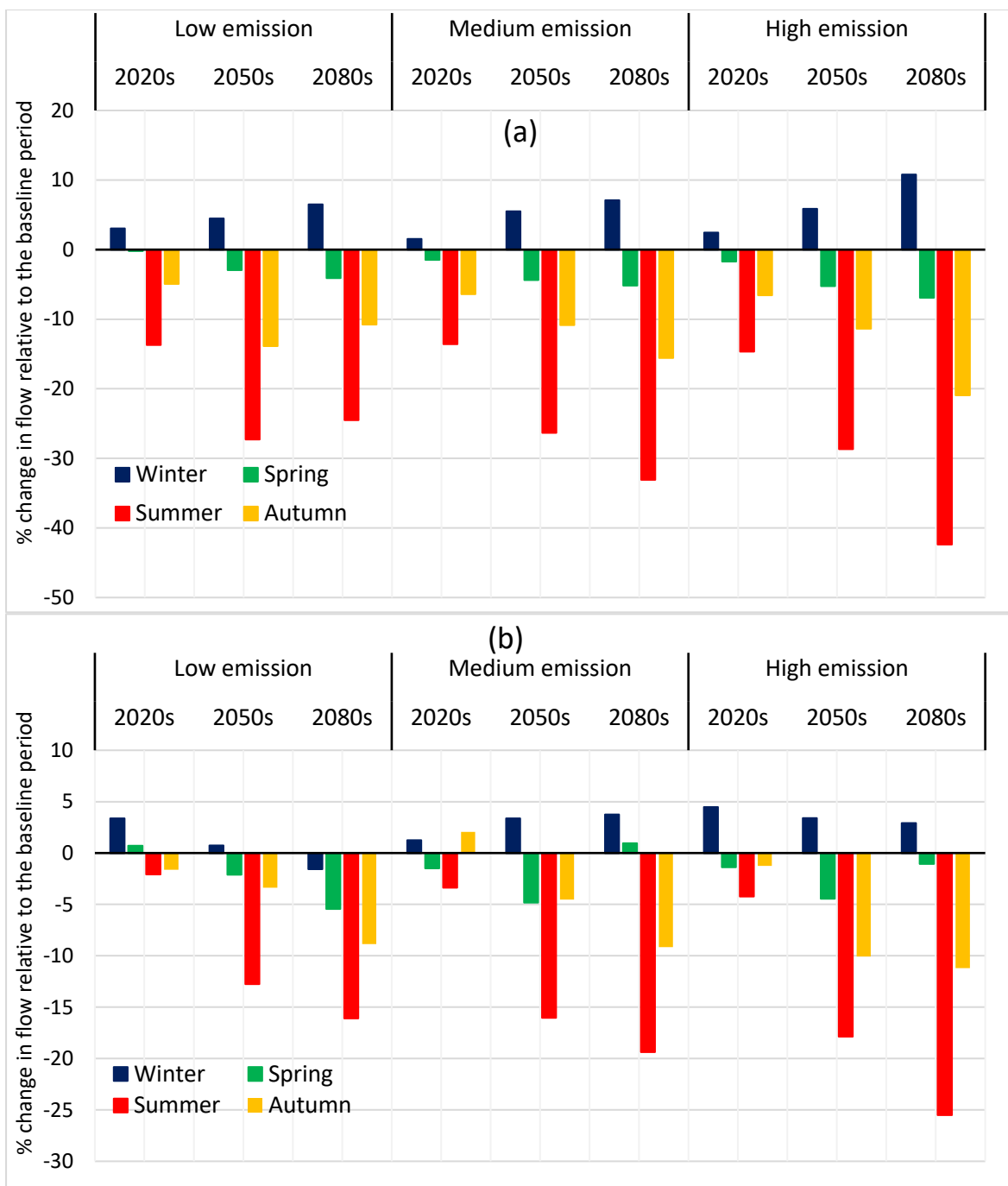
Figure 10: Percentage change in streamflow relative to the baseline period (1961-1990) over seasonal scale under low, medium and high emission scenarios for the 2020s, 2050s and 2080s, under UKCP09 joined probability (a) and under UKCP09 weather generator (b).

In autumn, streamflow is likely to decrease slightly under low and high emission scenarios, and a slight increase under medium emission scenarios in the 2020s. Overall, there is not much variation among the emission scenarios in the 2020s. However, in 2050s, more significantly under medium and high emission scenarios, up to 10% decrease under both joint probability and the weather generator approach

482   was observed. No significant change in rainfall is projected under medium and high emission scenarios,

483   but an increase in temperature and reduced rainfall in summer would lead to higher soil moisture deficit

484   during both the summer and autumn seasons, combined by an increase in autumn temperature this

485   would result in reduced streamflow in autumn due to higher water losses by evapotranspiration. The

486   simplified change factor (joint probability) showed slightly higher change compared to the weather

487   generator as joint probability method only consider two climate variables (rainfall and the temperature).

488   Overall, in all seasons, the severity of the change in streamflow more particularly during the summer

489   season could lead to very low stream flows, possibly leading to a high risk of inadequate domestic,

490   industrial and agricultural water supply. The latter is more significant for the Don catchment as there

491   are twenty-three reservoirs within the catchment, which significantly contribute to the water supply

492   systems.

493   *4.3.2. Changes in groundwater recharge*

494   The analysis using the weather generator and joint probability, under all emission scenarios and for the

495   selected time periods showed that the groundwater recharge would decrease, with some exceptions

496   under weather generator in the 2020s more significantly under high emission scenarios when

497   groundwater recharge increased by 4.32% compared to the baseline period (Fig. 11b). The increase in

498   winter precipitation would be counterbalanced by the higher water losses by the increased

499   evapotranspiration (due to increased temperature) which resulted in a small increase in groundwater

500   recharge in comparison to the baseline period in the 2020s. The groundwater recharge projections under

501   joint probability suggest that the groundwater recharge is likely to decrease from 3.39 to 11.25% under

502   all emission scenarios during the winter months (December, January, and February). Without exception,

503   groundwater recharge decreased for the three selected time periods, but the decrease will be slightly

504   less under low emission scenarios, compared to the medium and high emission. This is due to a smaller

505   increase in precipitation under low emission scenarios. Considering the change in precipitation under

506   all emission scenarios, the likely increase in the groundwater recharge is lower than expected, due to

507   losses by evapotranspiration that causes a decrease in stream flow and groundwater recharge in all

508   seasons. Other factor which could reduce the groundwater recharge in all seasons, is that the winter

509   precipitation is expected to come as extreme events and over a short period of time, as reported in

510   Alexander et al. (2005). The groundwater recharge is also likely to decrease in spring due to milder

511   increase in spring temperature and the insignificant change in precipitation.

512   A significant decrease in groundwater recharge is projected in summer months due to increasing

513   temperature and a decrease in precipitation, which result in higher water losses due to

514   evapotranspiration, higher soil moisture deficit and lower the groundwater recharge. Using joint

515   probability, the groundwater recharge is likely to decrease by over 60% under medium emission

516   scenarios in the 2080s and up to 75% under high emission scenarios. The percentage change in

517   groundwater recharge was not that high when using the weather generator data. The highest decrease

518   in summer groundwater recharge projected for the 2080s is likely to be over 40%, compared to the

519   baseline period. Such a significant decrease in groundwater recharge could be the result of increased

520   soil moisture deficit. Under all emission scenarios and observed time periods, the groundwater recharge

521   is likely to decrease by -38% to -58% under joint probability and -10% to -30% under the weather

522   generator under the low emission scenarios; while under medium emission scenarios the decrease in

523   groundwater recharge would fall within -38% to -67% with joint probability and -13% to -35% with

524   the weather generator; the highest decrease is projected under high emission scenarios with -39% to -

525   76% under joint probability and -13% to -40.2% under the weather generator, all changes are in

526   comparison to the baseline period.
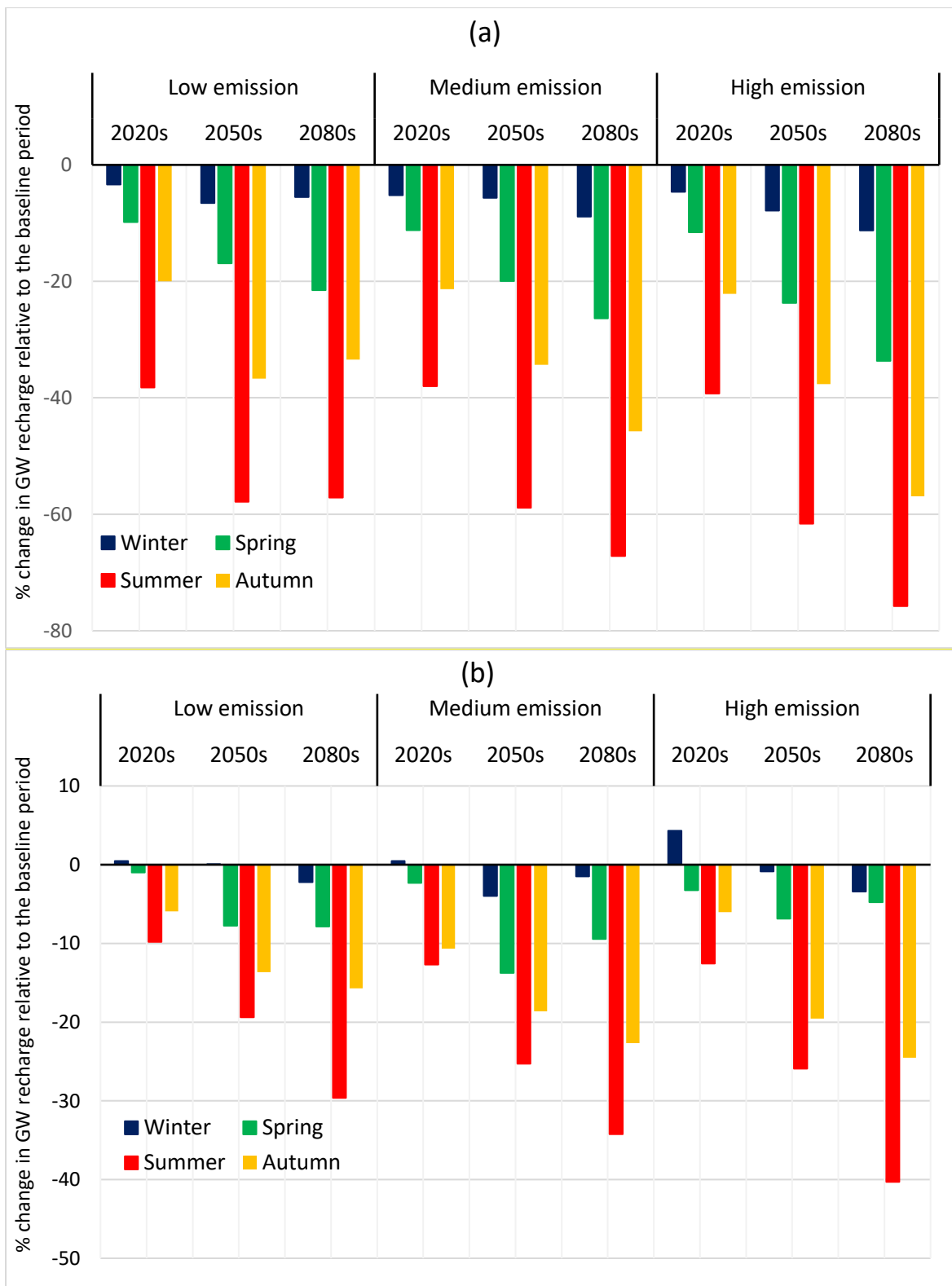

527

528

529
530 **Figure 11:** Percentage change in groundwater recharge in the Don Catchment for the different seasons

531 over a selected time period, based on joint probability (a) and Weather Generator (b) of UKCP09 under

532 different climate change scenarios.

533   In summer months (June, July, August) enhanced evapotranspiration, together with the decreased

534   precipitation, would result in reduced streamflow and groundwater recharge. Higher evapotranspiration

535   combined with lower rainfall during the summer months would result in an increase in soil moisture

536   deficit, which would result in low groundwater recharge during the autumn months under all emission

537   scenarios. However, the severity of the decrease is much higher in the second half of the century under

538   high emission scenarios. Under low emission scenarios the groundwater recharge is likely to decrease

539   by -2.15% to -12%, under medium emission the likely decrease will be within the -5.93% to -14.87%

540   range and under high emission scenarios the projected likely decrease will be within -3.99% to -25.77%

541   range. The higher decrease in groundwater recharge under high emission scenarios would result due to

542   the increase in soil moisture deficit during the summer months. Studies carried out in the Midlands

543   suggest that maintaining water supplies in the 2050s may be challenging due to the limited availability

544   of the water resources (Wade et al., 2013), suggesting that demand-side measures would be required to

545   match the future water supplies availability (Wade et al., 2013).

546   *4.3.3. Drought indices*

547   To investigate the impact of climate change, a number of drought indices including soil moisture deficit,

548   wetness index of the root-zone, and reconnaissance drought index were considered. As a result of the

549   drier and warmer climatic conditions, higher water losses by the evapotranspiration, higher soil

550   moisture deficit and low Wetness index were observed (Fig. 12). To illustrate the impact of decreasing

551   rainfall and increasing water losses due to the evapotranspiration, the standardized reconnaissance

552   drought index, *RDI* was applied. The adjusted RDI was calculated from the net rainfall and actual

553   evapotranspiration of the selected time periods: 2020s, 2050s and 2080s for three emission scenarios

554   (Fig 13). The analysis revealed an increase in number of moderate and severe drought events, more

555   importantly under the medium and high emission scenarios. In comparison to the baseline period, the

556   extreme drought events are likely to double in the later part of the century. Not only the extreme dry

557   events but also, severe drought events are also likely to increase in the future. In addition, the frequency

558   of moderately droughts events (RDI -1 to -1.5) is likely to increase in the future, more specifically under

559   medium and high emission scenarios.

560
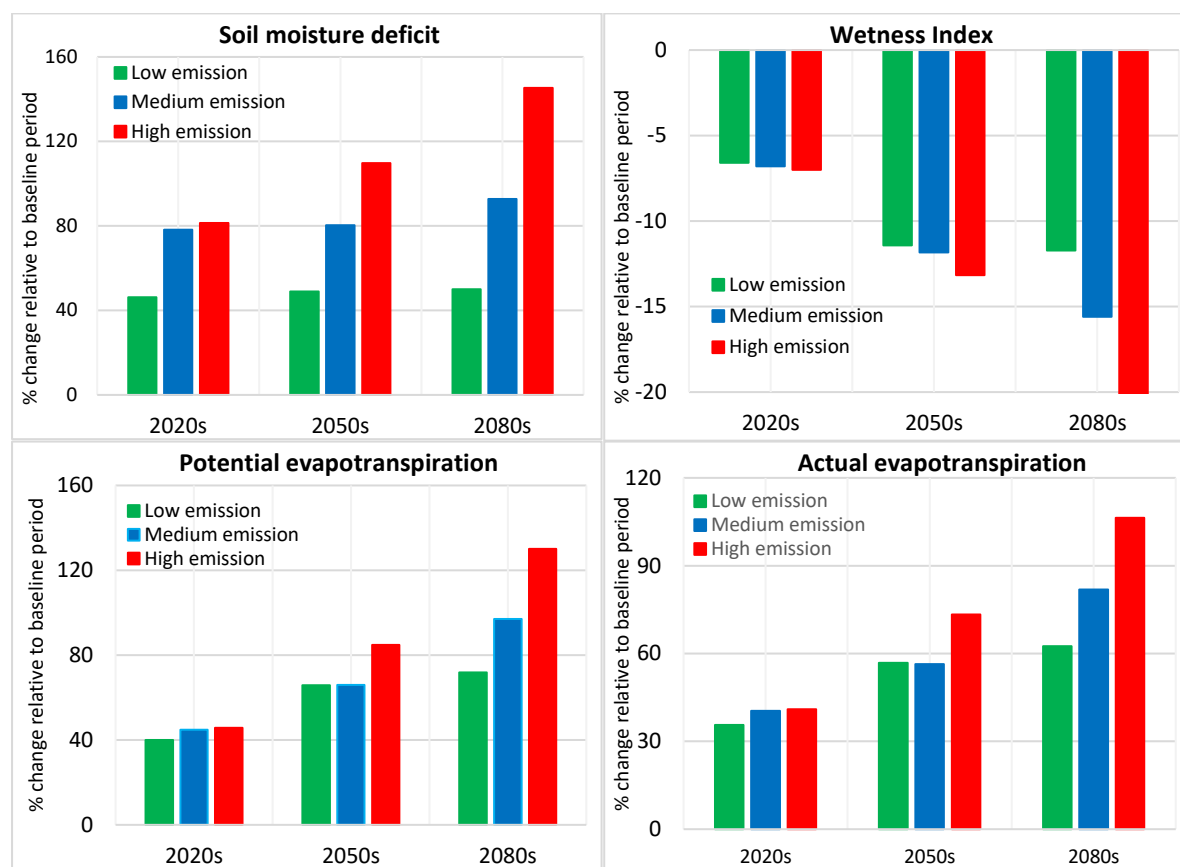
561
562   **Figure 12:** Seasonal changes in soil moisture deficit, actual evapotranspiration and the wetness index

563   of the root zone for the Don Catchment under all emission scenarios base on UKCP09 joint probability.

564

565
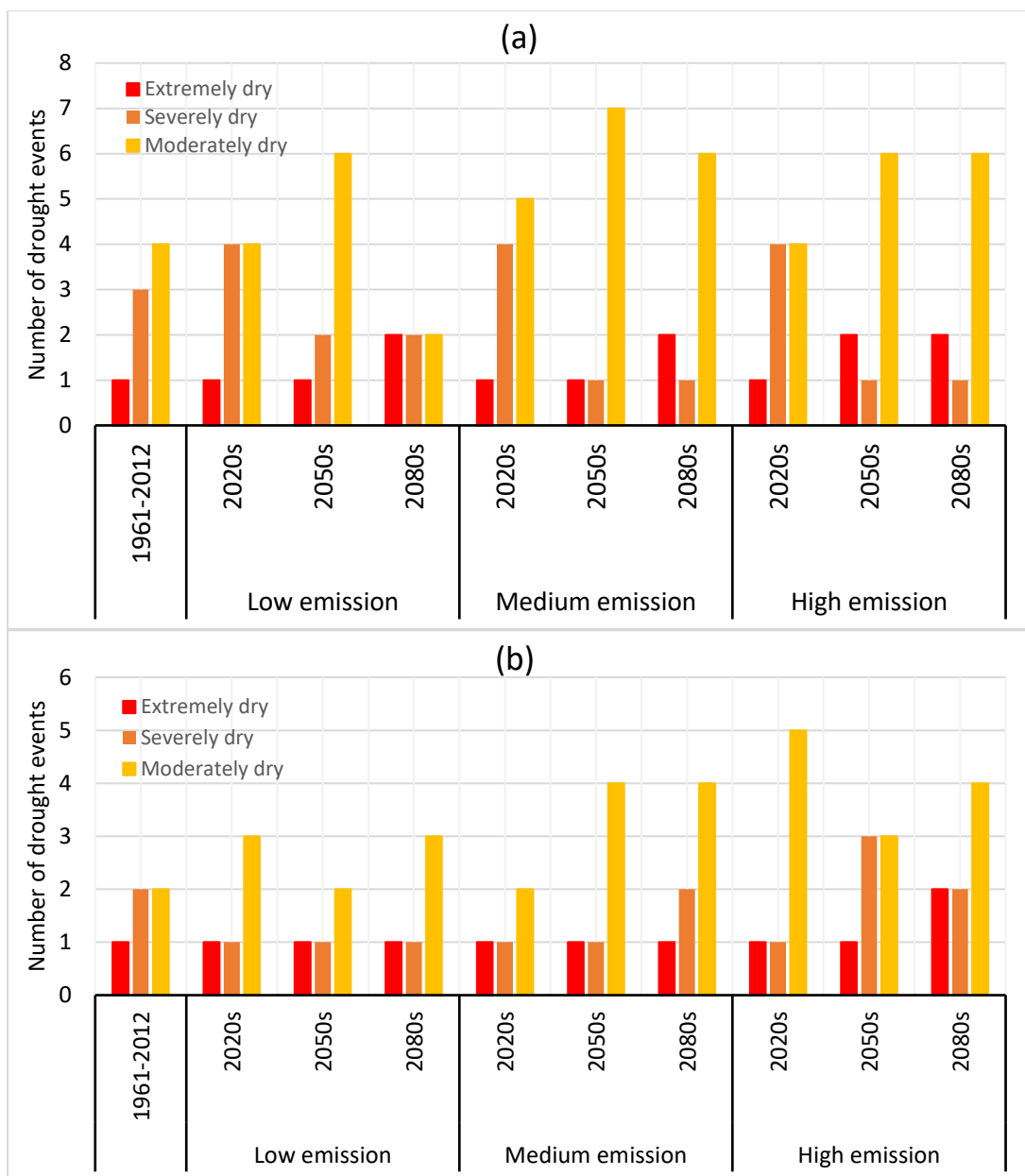
566
567 **Figure 13:** The severity of drought events observed in the Don Catchment under the three emission

568 scenarios for the 2020s, 2050s and 2080s (a) under joint probability and using the weather generator

569 data (b).

570   *4.3. Impacts of land use changes on the water resources*

571 To study the impact of land use changes on the water balance a number of possible plausible and

572 hypothetical land scenarios were examined (Table 3). The number of tested possible and hypothetical

573 land use changes and the impacts are:

574   1.   100% Grass area replaced by winter barley: Stream flow is likely to increase between 3% and 6%

575   while groundwater recharge is likely to increase between 1 and 7%.

576   2.   Grass area replaced by oil seed rape: Stream flow is likely to decrease by up to 3% in all seasons apart

577   from autumn where it is likely to slightly increase by <3%, while groundwater is likely to decrease

578   between ~ 2% apart from autumn where the recharge is likely to increase by ~2%.

579   3.   40% urban expansion replacing grass and arable area: Stream flow is likely to increase by ~1% and

580   groundwater recharge by ~2%.

581   4.   Replacing 50% of winter barley by oil seed rape: Stream flow is likely to decrease by ~2% and

582   groundwater recharge by ~3%

583   5.   Whole catchment as grass area: Stream flow is likely to decrease by ~2% and 8% and groundwater

584   recharge by ~5% and 9%.

585   6.   Whole catchment as Broad leaf forest area: The stream flow is likely to decrease between 9% and 17%

586   and groundwater recharge between 10% and 22%.

587   The expansion of the wooded broadleaf forest would be likely to result in an increase of soil moisture

588 deficit, more specifically during the spring and summer seasons when plants at maximum growth rate

589 and take up much of water and transpiration rates are significant. Urban expansion could result in

590 increased streamflow (likely to increase in flood risk) and increase in groundwater recharge.

591 Increasing conventional crops, like barley replacing grass could result in a slight increase in river flow

592 and a decrease in soil moisture deficit, compared with oilseed rape, which takes up more water during

593 the spring season (Table 3).

594 Sensitivity analysis to see the combined effect of both climate and land use changes revealed that

595 overall, the effect of the land use changes on the hydrological variables was much less than the effect

596 of climate change. Considering the possible changes in climatic variables and extreme events in the

597 future, sustainable land use practices could potentially be used to mitigate the impact of climate

598 change as the studied catchment is of significance for the water supplies in the Sheffield area

599

600

601

602

603   **Table 3:** Impact of land use changes in the Don Catchment on stream flow and groundwater recharge.

Hydrological variables	Land use types		100% Grass area replaced by winter barley	Grass area replaced by oil seed rape	40% urban expansion replacing grass and arable area	Replacing 50% of winter barley by oil seed rape	Whole catchment as grass area	Whole catchment as Broad leaf forest area
River flow	Season	%	% change	% change	% change	% change	% change	% change
	Winter	6.46	-2.8	1.14	-1.35	-2.64	-12.4
	Spring	6.10	-1.2	1.13	-0.50	-5.22	-16.6
	Summer	3.39	-0.31	0.42	-0.10	-8.35	-14.4
	Autumn	3.57	2.4	-0.05	-1.14	-3.90	-9.01
Groundwater recharge	Winter	6.53	-2.01	1.40	-0.47	-7.80	-13.48
	Spring	5.21	-0.05	1.90	0.30	-6.10	-15.21
	Summer	0.60	-1.95	1.40	0.58	-9.10	-21.90
	Autumn	6.48	3.91	1.80	-3.13	-5.30	-9.65

604

605

606

607

608

609

610

611

612

613

614

615

616

617   **5. Discussion**

618   The drought indices used in the study were able to identify all the historical drought events. The adjusted

619   reconnaissance drought index calculated using the actual evapotranspiration and the net rainfall, in

620   addition, to the conventional *RDI*, *SPI/SPEI*, *SMD* and *WI* of the root-zone were used as indicators to

621   identify future drought events. The standardized precipitation index, *SPI/SPEI* indicated the

622   significantly negative deviation from the average precipitation in the 1970s, specifically in 1975-1976

623   and 1995-1996. The 1975/1976 drought has been studied in a number of studies including (Perry, 1976,

624   Marsh et al., 2007). During the 1995/1996 drought period, water resources in the Northern England and

625   in the Midlands remained fragile as April to November 1995 rainfall was the second lowest in the 228

626   years for England and Wales (Marsh and Turton, 1996). All the applied drought indices including

627   reconnaissance drought index (*RDI*), soil moisture deficit, *SMD* and the Wetness index, *WI* of the root-

628   zone (Figures 7-9) identified these drought events. During these drought events, the *RDI*, *SPI*/*SPEI*

629   were well below -2, which identifies them as 'extreme drought' events (caused by extremely low rainfall

630   and high evapotranspiration). Under current land use practices, a further increase in likelihood of

631   extreme drought events, specifically under medium and high emission scenarios in the middle and the

632   latter part of the century (Figure 13) due to an increase in temperature, resulting in higher water losses

633   by evapotranspiration, a decrease in rainfall, an increase in soil moisture deficit consequently would

634   result in more frequent and severe drought in the future. This would further increase the pressure on

635   water resources due to changes in land use practices.

636   The land use type would significantly change in the future, especially due to urbanisation, as

637   urbanisation would further increase pressure on water resources in the Don catchment. The other key

638   land use changes are the agricultural land use practices, which are driven by the farmers' decisions

639   which are market based, as well as the availability of investment, subsidies and the socio-cultural

640   attributes of individual farmers. Increasing woodland area would significantly reduce both stream flow

641   and groundwater recharge.

642   The application of a wider range of drought indices could be used to identify different types of droughts.

643   For example, in agriculture, when soil moisture deficit, *SMD* or Wetness Index, *WI* of the root zone,

644   reach a critical level, crops will require irrigation, particularly during the summer months. This will

645   require reliable water supplies to secure adequate yield. The *WI* value, if close to 1, would indicate a

646   wet catchment with a possible runoff generation during the next rainfall event, therefore, it is a help to

647   reservoir managers to know the *WI* in real time. *RDI* would be helpful for short and long-term planning

648   by water authorities and water companies. Therefore, the findings from the modelling work could be

649   used to review the future surface water abstraction regulations to be in line with the water resources

650   availability as predicted by the hydrological models and in possible planning of building new water

651   infrastructure to increase the water storage in relation to increasing future water demand.

652   The DiCaSM model proved to be a good tool to predict river flow and recharge to groundwater and can

653   simulate the effects of climate change on the different elements of the hydrological cycle. The future

654   climate change scenarios suggested a significant decrease in groundwater recharge although climate

655   models project an increase in winter rainfall but such increase could be counter balanced by an increase

656   in evapotranspiration and increase of soil moisture deficit during the summer and autumn seasons. The

657   streamflow decrease would affect the Don catchment more as there are 23 reservoirs within the

658   catchment, which are recharged during the winter season. Considering the possible decrease in

659   groundwater recharge and streamflow and the increasing possibility of droughts in the future. New

660   investment will be required if water demand is not met through greater water use efficiency or by

661   alternative sources to traditional reservoirs, such as rainwater harvesting systems (Zhang and Hu, 2014)

662   or by reducing evaporation from the reservoirs by for example, floating solar panels, spreading

663   ecologically friendly agents on water surface or an ultra-thin layer of organic molecules on their surface

664   (Alamaro et al., 2012). The implication of surface water abstractions during drought and low flow

665   periods would reduce river flows possibly below the minimum environmental flow. Alternatively,

666   restrictions on abstraction to maintain the minimum environmental flows may restrict crop yields and

667   food production.

6. Conclusion

The model calibration and validation results showed a good agreement between the observed the simulated flow and overall model efficiency using the *NS* index was above 82% for the 52 years' study period. In addition to the stream flow, the DiCaSM hydrological model identified all drought events using the drought indices: *RDI*, *SMD,* and the *WI* in the 1970s but also during the 1980s, 1990s and the most recent ones in 2010-2012. The analysis revealed that the standard *RDI,* based on gross rainfall and potential evapotranspiration*,* showed slightly higher severity than the adjusted *RDI*. The latter is based on realistic input of net rainfall (excluding interception losses by vegetation cover) and actual evapotranspiration, which reflects the actual losses from soil and plants. Under the UKCP09 climate change projection, the streamflow and the groundwater recharge significantly decreased, more specifically during the summer months, while the severity of the drought events significantly increased over time. All the applied drought indices (*SMD*, *WI*, and *RDI*) identified an increase in the severity of the drought under future climatic change scenarios. Under high emission scenarios, the severity was higher as this severity was associated with the increasing temperature and subsequently increasing water losses by evapotranspiration, thus reducing soil moisture availability, surface runoff to streams and recharge to groundwater. These findings would help in planning for perhaps extra water infrastructure work if needed, such as building more reservoirs or water transfer pipelines from water-rich to water-poor regions and planning for irrigation water demand under different climatic conditions. The study catchment is of significance as there are twenty-three reservoirs in the catchment boundary, which significantly contribute into the water supply of the catchment. The findings of this study can also be useful in revising the "Catchment Abstraction Management Strategies, CAMS" for the Don catchment.

694 Advisory Group meetings for the Don catchment. The authors would like to acknowledge the data

695 sources: Background mapping from Ordnance Survey ('1:250 000 Scale Colour Raster'). Catchment

696 boundary and gauging station location data from Centre for Ecology and Hydrology (Morris et al., 1990,

697 Morris and Flavin, 1994). River and waterbody data from Centre for Ecology and Hydrology ('Digital

698 Rivers 50km GB' Web Map Service). Land cover data from Centre for Ecology and Hydrology (Land

699 Cover Map 2007 (25m raster, GB) Web Map Service (Morton et al., 2011). Standardized Precipitation

700 Index time series for IHU groups (1961-2012) [SPI_IHU_groups] data licensed from NERC Centre for

701 Ecology & Hydrology. Soils data courtesy of Cranfield University (1:250 000 Soilscapes for England

702 and Wales Web Map Service). Hydrogeology data from British Geological Survey (DiGMapGB 1:625

703 000 scale digital hydrogeological data).

704 **References:**

705 AFZAL, M., GAGNON, A. S. & MANSELL, M. G. 2015. The impact of projected changes in climate
706   variability on the reliability of surface water supply in Scotland. *Water Science and*
707   *Technology: Water Supply,* 15**,** 736-745.
708 ALAMARO, M., EMANUEL, K. & LANGER, R. S. 2012. Surface film distribution system and
709   method thereof. Google Patents.
710 ALEXANDER, L. V., TETT, S. F. & JONSSON, T. 2005. Recent observed changes in severe storms
711   over the United Kingdom and Iceland. *Geophysical Research Letters,* 32.
712 ALLEN, R. G., PEREIRA, L. S., RAES, D. & SMITH, M. 1998. Crop evapotranspiration-Guidelines
713   for computing crop water requirements-FAO Irrigation and drainage paper 56. *Fao, Rome,* 300**,**
714   D05109.
715 BACHMAIR, S., TANGUY, M., HANNAFORD, J. & STAHL, K. 2018. How well do meteorological
716   indicators represent agricultural and forest drought across Europe? *Environmental Research*
717   *Letters,* 13**,** 034042.
718 BENTO, V. A., GOUVEIA, C. M., DACAMARA, C. C. & TRIGO, I. F. 2018. A climatological
719   assessment of drought impact on vegetation health index. *Agricultural and Forest Meteorology,*
720   259**,** 286-295.
721 BURKE, E. J., PERRY, R. H. & BROWN, S. J. 2010. An extreme value analysis of UK drought and
722   projections of change in the future. *Journal of Hydrology,* 388**,** 131-143.
723 CEH. 2014. *CEH digital river network of Great Britain web map service* [Online]. Available:
724   https://data.gov.uk/dataset/3c7ea82e-83e0-45a3-9a3f-8ba653b3211b/ceh-digital-river-
725   network-of-great-britain-web-map-service [Accessed 2014].
726 CROPPER, T. E. & CROPPER, P. E. 2016. A 133-year record of climate change and variability from
727   Sheffield, England. *Climate,* 4**,** 46.
728 DE CÁCERES, M., MARTIN-STPAUL, N., TURCO, M., CABON, A. & GRANDA, V. 2018.
729   Estimating daily meteorological data and downscaling climate models over landscapes.
730   *Environmental Modelling & Software,* 108**,** 186-196.
731 FORESTIERI, A., ARNONE, E., BLENKINSOP, S., CANDELA, A., FOWLER, H. & NOTO, L. V.
732   2018. The impact of climate change on extreme precipitation in Sicily, Italy. *Hydrological*
733   *Processes,* 32**,** 332-348.
734 FOWLER, H. & KILSBY, C. 2002. A weather-type approach to analysing water resource drought in
735   the Yorkshire region from 1881 to 1998. *Journal of Hydrology,* 262**,** 177-192.

736 GUDMUNDSSON, L., BREMNES, J., HAUGEN, J. & ENGEN-SKAUGEN, T. 2012. Downscaling
737   RCM precipitation to the station scale using statistical transformations-a comparison of
738   methods. *Hydrology and Earth System Sciences,* 16**,** 3383.
739 GUPTA, H. V., KLING, H., YILMAZ, K. K. & MARTINEZ, G. F. 2009. Decomposition of the mean
740   squared error and NSE performance criteria: Implications for improving hydrological
741   modelling. *Journal of Hydrology,* 377**,** 80-91.
742 HAKALA, K., ADDOR, N. & SEIBERT, J. 2018. Hydrological Modeling to Evaluate Climate Model
743   Simulations and Their Bias Correction. *Journal of Hydrometeorology,* 19**,** 1321-1337.
744 HOUGH, M., PALMER, S., WEIR, A., LEE, M. & BARRIE, I. 1997. The Meteorological Office
745   rainfall and evaporation calculation system: MORECS version 2.0 (1995). *An update to*
746   *hydrological memorandum,* 45**,** 80.
747 JACKSON, C. R., BLOOMFIELD, J. P. & MACKAY, J. D. 2015. Evidence for changes in historic
748   and future groundwater levels in the UK. *Progress in Physical Geography,* 39**,** 49-67.
749 KALMA, J., BATES, B. & WOODS, R. 1995. Predicting catchment-scale soil moisture status with
750   limited field measurements. *Hydrological processes,* 9**,** 445-467.
751 KRAUSE, P., BOYLE, D. & BÄSE, F. 2005. Comparison of different efficiency criteria for
752   hydrological model assessment. *Advances in geosciences,* 5**,** 89-97.
753 KUNZ, J., LÖFFLER, G. & BAUHUS, J. 2018. Minor European broadleaved tree species are more
754   drought-tolerant than Fagus sylvatica but not more tolerant than Quercus petraea. *Forest*
755   *Ecology and Management,* 414**,** 15-27.
756 MARSH, T., COLE, G. & WILBY, R. 2007. Major droughts in England and Wales, 1800–2006.
757   *Weather,* 62**,** 87-93.
758 MARSH, T. & GREEN, S. 1997. UK hydrological review 1997. 2nd ed.: Centre for Ecology and
759   Hydrology.
760 MARSH, T. & TURTON, P. 1996. The 1995 drought—a water resources perspective. *Weather,* 51**,** 46-
761   53.
762 MCKEE, T. B., DOESKEN, N. J. & KLEIST, J. The relationship of drought frequency and duration to
763   time scales. Proceedings of the 8th Conference on Applied Climatology, 1993. American
764   Meteorological Society Boston, MA, 179-183.
765 MORRIS, D. & FLAVIN, R. 1994. Sub-set of the UK 50 m by 50 m hydrological digital terrain model
766   grids. *NERC, Institute of Hydrology, Wallingford*.
767 MORRIS, D., FLAVIN, R. & MOORE, R. 1990. *A digital terrain model for hydrology*.
768 MORTON, D., ROWLAND, C., WOOD, C., MEEK, L., MARSTON, C., SMITH, G.,
769   WADSWORTH, R. & SIMPSON, I. 2011. Final Report for LCM2007-the new UK land cover
770   map. Countryside Survey Technical Report No 11/07.
771 NASH, J. E. & SUTCLIFFE, J. V. 1970. River flow forecasting through conceptual models part I—A
772   discussion of principles. *Journal of hydrology,* 10**,** 282-290.
773 NRFA. 2014. *National River flow Archive* [Online]. Available: http://nrfa.ceh.ac.uk/ [Accessed 2014].
774 PARRY, S., WILBY, R. L., PRUDHOMME, C. & WOOD, P. J. 2016. A systematic assessment of
775   drought termination in the United Kingdom.
776 PERRY, A. 1976. The long drought of 1975–76. *Weather,* 31**,** 328-336.
777 RAGAB, R. & BROMLEY, J. 2010. IHMS—Integrated Hydrological Modelling System. Part 1.
778   Hydrological processes and general structure. *Hydrological processes,* 24**,** 2663-2680.
779 RAGAB, R., BROMLEY, J., DÖRFLINGER, G. & KATSIKIDES, S. 2010. IHMS—Integrated
780   Hydrological Modelling System. Part 2. Application of linked unsaturated, DiCaSM and
781   saturated zone, MODFLOW models on Kouris and Akrotiri catchments in Cyprus.
782   *Hydrological processes,* 24**,** 2681-2692.
783 ROBINSON, E., BLYTH, E., CLARK, D., COMYN-PLATT, E., FINCH, J. & RUDD, A. 2015.
784   Climate hydrology and ecology research support system potential evapotranspiration dataset
785   for Great Britain (1961-2015)[CHESS-PE].
786 ROUNSEVELL, M. & REAY, D. 2009. Land use and climate change in the UK. *Land Use Policy,* 26**,**
787   S160-S169.
788 SENEVIRATNE, S. I. 2012. Climate science: Historical drought trends revisited. *Nature,* 491**,** 338.

789   SHIFERAW, B. A., OKELLO, J. & REDDY, R. V. 2009. Adoption and adaptation of natural resource
790   management innovations in smallholder agriculture: reflections on key lessons and best
791   practices. *Environment, development and sustainability,* 11**,** 601-619.
792   SOLANDER, K. C. & WILSON, C. J. 2018. The Cape Town drought: what is happening and will it
793   happen again? : Los Alamos National Lab.(LANL), Los Alamos, NM (United States).
794   SPRAGGS, G., PEAVER, L., JONES, P. & EDE, P. 2015. Re-construction of historic drought in the
795   Anglian Region (UK) over the period 1798–2010 and the implications for water resources and
796   drought management. *Journal of hydrology,* 526**,** 231-252.
797   TANGUY, M., DIXON, H., PROSDOCIMI, I., MORRIS, D. & KELLER, V. 2016. Gridded estimates
798   of daily and monthly areal rainfall for the United Kingdom (1890–2015)[CEH-GEAR]. *NERC*
799   *Environmental Information Data Centre, doi,* 10.
800   THE_DON_NETWORK. 2018. *Our plan for the River Don* [Online]. Available: https://dcrt.org.uk/wp-
801   content/uploads/2013/05/6541-1+Don+Network+Report+lo+res.pdf   [Accessed   24/10/2018
802   2018].
803   THORNTHWAITE, C. W. 1948. An approach toward a rational classification of climate. *Geographical*
804   *review,* 38**,** 55-94.
805   TIRIVAROMBO, S., OSUPILE, D. & ELIASSON, P. 2018. Drought monitoring and analysis:
806   Standardised Precipitation Evapotranspiration Index (SPEI) and Standardised Precipitation
807   Index (SPI). *Physics and Chemistry of the Earth, Parts A/B/C*.
808   TSAKIRIS, G., PANGALOU, D. & VANGELIS, H. 2007. Regional drought assessment based on the
809   Reconnaissance Drought Index (RDI). *Water resources management,* 21**,** 821-833.
810   VANGELIS, H., TIGKAS, D. & TSAKIRIS, G. 2013. The effect of PET method on Reconnaissance
811   Drought Index (RDI) calculation. *Journal of Arid Environments,* 88**,** 130-140.
812   VICENTE-SERRANO, S. M., BEGUERÍA, S. & LÓPEZ-MORENO, J. I. 2010. A multiscalar drought
813   index sensitive to global warming: the standardized precipitation evapotranspiration index.
814   *Journal of climate,* 23**,** 1696-1718.
815   WADE, S. D., RANCE, J. & REYNARD, N. 2013. The UK climate change risk assessment 2012:
816   assessing the impacts on water resources to inform policy makers. *Water Resources*
817   *Management,* 27**,** 1085-1109.
818   WANG, H., TETZLAFF, D. & SOULSBY, C. 2018. Modelling the effects of land cover and climate
819   change on soil water partitioning in a boreal headwater catchment. *Journal of Hydrology,* 558**,**
820   520-531.
821   WANG, L. & CHEN, W. 2014. A CMIP5 multimodel projection of future temperature, precipitation,
822   and climatological drought in China. *International Journal of Climatology,* 34**,** 2059-2078.
823   WILBY,   R.   L.,   PRUDHOMME,   C.,   PARRY,   S.   &   MUCHAN,   K.   2015.   Persistence   of
824   hydrometeorological droughts in the United Kingdom: A regional analysis of multi-season
825   rainfall and river flow anomalies. *Journal of Extreme Events,* 2**,** 1550006.
826   ZARCH, M. A. A., SIVAKUMAR, B. & SHARMA, A. 2015. Droughts in a warming climate: A global
827   assessment of Standardized precipitation index (SPI) and Reconnaissance drought index (RDI).
828   *Journal of Hydrology,* 526**,** 183-195.
829   ZHANG, X. & HU, M. 2014. Effectiveness of rainwater harvesting in runoff volume reduction in a
830   planned industrial park, China. *Water resources management,* 28**,** 671-682.

831